Check for updates

Current state of the heavy metal pollution, microbial diversity, and bioremediation experiments around the Qixia Mountain lead–zinc mine in Nanjing, China†

Xiaofang Li,[ab] Xiaochi An,[b] Kairui Jiao,[b] Haoqin Pan[a] and Bin Lian [iD] *[b]

The extraction and processing of ores from lead–zinc mines, coupled with the disposal of tailings, often result in severe environmental contamination that poses significant ecological and public health risks, demanding urgent attention and action. In this study, field investigations and analyses were performed to evaluate the state of heavy metal pollution and microbial diversity in the soil around Qixia Mountain lead–zinc mine in Nanjing, China. The effect of plant-/microorganism-induced mineralization on the remediation of the contaminated soil was studied *via* pot experiments. Results indicated serious soil pollution around the mine, and dominant bacterial species (*e.g. Sphingomonas*) in different soil environments exhibited high resistance to heavy metals. Pot experiments showed that amaranth-/ *Bacillus velezensis*-induced mineralization can significantly reduce the heavy metal pollution levels (Nemerow pollution index decreased from 4.5 to about 1.0) in soil. This study reveals the profound impacts of mining activities on soil ecology and human health, providing a theoretical basis for the prevention and control of soil pollution in farmlands surrounding lead–zinc mines.

1. Introduction

Mining of metals has a great impact on the geological environment around mines, which can lead to pollution of the surface soil and groundwater system and even a decline in the quality of the surrounding air.[1,2] Depending on the chemical composition of the ore, the main sources of heavy metal pollution arise from the ore mining process itself, accumulation of tailings, and chemicals used in flotation tanks.[3,4] The chemicals used in mineral processing generally remain in the soil and water of abandoned mines for a long time, causing serious environmental damage. For example, strong acids (*e.g.* HNO$_3$ and HCl) are often used to leach and concentrate zinc ores. The subsequent volatilization of this acidic liquor can easily produce a large amount of irritating vapor to diffuse into the surrounding air.[5] Any leakage of this acidic liquor can also directly lead to soil acidification and hardening.[6,7] Some metallic elements present in newly exposed ores can also chemically react with rainwater and air, producing substances

that may well be harmful to the human body and environment.[8,9] The long-term accumulation of tailings from lead–zinc mines can produce a large number of harmful gases and migratable forms of heavy metal compounds, resulting in various pollutants entering the soil, air, and water.[8,9] Mining activity can thus lead to heavy metals reaching farmlands near the mine, which clearly poses a direct risk to any vegetables and crops planted there. Therefore, heavy metal pollution around mines should be continuously monitored, and precautionary steps should be implemented to prevent the large-scale diffusion of such pollutants into the local ecological environment. At present, the heavy metal pollution levels in the soil, air, and water sources in mining areas are mainly assessed using pollution indices and *via* the construction of risk assessment models. The comprehensive Nemerow pollution index is the most commonly used evaluation standard in this regard.[10]

Mining activities not only pollute the environment of the mining area and its surroundings, but also change the community structure of microorganisms in the soil.[11] Previous studies have found that the dominant bacteria in the soil of lead–zinc mining area are mainly actinomycetes, proteobacteria, and acidobacteria; the most widely distributed fungi are Ascomycetes.[12] In the soil of copper mining areas, the most widely distributed bacteria are Proteobacteria and Firmicutes.[13] In view of the heavy metal pollution in soil caused by mining activities, plant–microorganism combined remediation is often used for pollution control. For example, plants combined with

[a] Shandong Provincial University Laboratory for Protected Horticulture, Shandong Facility Horticulture Bioengineering Research Center, Weifang University of Science and Technology, Weifang, 262700, China

[b] College of Life Sciences, College of Marine Science and Engineering, Nanjing Normal University, Nanjing, 210023, China. E-mail: bin2368@vip.163.com; Fax: +86 025 85898551; Tel: +86 025 85898551

† Electronic supplementary information (ESI) available. See DOI: https://doi.org/10.1039/d4ra07920e

Stenotrophomonas sp. can be used to effectively repair soil contaminated with uranium.[14] Furthermore, a combination of *Bacillus megaterium* and *B. licheniformis* with *Arabidopsis thaliana* can repair cadmium- and zinc-contaminated soil.[15] The fungus *Penicillium janthinellum* combined with plants can also be used to repair cadmium-contaminated soil.[16] In this case, the addition of the fungus to heavy metal-contaminated soil was found to promote the growth of the plants, and hence, the absorption of cadmium. In short, the method of plant–microorganism synergistic remediation to improve the soil environment of mines has received extensive attention. However, due to the great differences in different regions and types of mine environments, it is still necessary to explore the bioremediation methods suitable for the local environment.

The polymetallic Qixia Mountain deposit is the largest lead–zinc–silver deposit in east China. The deposit has been mined over seventy years. The long-term mining and mineral processing of the metals have directly and indirectly caused serious pollution to the air and surrounding soil.[17] As a result, it has been reported that the farmland and scenic area around Qixia Mountain have become polluted by heavy metals such as lead, zinc, cadmium, and copper.[18] Due to the relatively large population density and various land use types around the Qixia Mountain lead–zinc mine, the vegetable field crops affected by mining are more likely to enter the market circulation, which brings hidden dangers to the food safety of the surrounding residents. In response, the local government has tried to strengthen the measures taken to protect the Qixia Mountain environment. The environment surrounding the mining area has consequently improved greatly over the past ten years. In order to reveal the current situation of soil pollution remediation around the Qixia Mountain lead–zinc mining area and solve the potential problems of vegetable field, this study focused on the mineral processing pond in the Qixia Mountain lead–zinc mining area and evaluated the soil heavy metal content, physical and chemical properties and microbial diversity distribution of different land use types (vegetable field, woodland, grassland, and around the mineral processing pond) around the mining area. Owing to the high levels of heavy metals in vegetable soil, a pot remediation experiment was conducted using local soil. This experiment provided a theoretical basis for the pollution control of lead–zinc mine environments and the bioremediation of heavy metal-contaminated farmland.

2. Materials and methods

2.1 Collection of soil samples

The Qixia Mountain lead–zinc mining area is located in Qixia District (N 32° 07′, E 118° 52′), Nanjing City, Jiangsu Province, with a humid climate in the northern subtropical zone, distinct four seasons, and abundant rainfall. The average rainfall is 1106 millimeters, and the annual average temperature is 15 °C. The samples were collected using the five-point sampling method, using a shovel to clean the plants on the surface, and then using a sterilized shovel to take soil at a depth of about 5–15 cm. After sampling, the soil was placed in a pre-prepared sterile sampling

bag, stored in dry ice, and quickly transported to the laboratory for storage at −80 °C. The mining area is centered around an open-pit mineral flotation tank. Furthermore, the mine is surrounded by land used for different purposes. This research focuses on soil from a vegetable field (VF), grassland (GL), and woodland (WL). The sampling sites are all located about 150 m from the mine.

In order to reveal the influence of the mine on the physical and chemical properties of the soil and the microorganisms therein, a soil sample was also taken from around the flotation tank in the mineral mining and separating area (Mining area, MA) itself. The soil samples VF, GL, WL, and MA constitute the experimental objects used in this work (Fig. 1). The samples were collected from fresh soil taken from 10–15 cm below the ground surface. In all, 4 sampling points were selected as replicates at each site, giving a total of 16 samples. Each sample collected was thoroughly mixed and divided into three parts. One was used to determine the physical and chemical properties of the soil. The second was used to determine the diversity of the bacteria and fungi in the soil (these samples were stored at −80 °C until required for use). The third was reserved for other subsequent experiments.

2.2 Determination of the physical and chemical properties of the soils

The 16 soil samples used were first air-dried. A portion (5.0 g) of soil that had been passed through a 10-mesh plastic sieve was weighed into a 50 mL beaker and mixed with 25 mL of CO_2-free water. The pH (PHSJ-4F, Shanghai Leici, China) and electrical conductivity (SX731, Shanghai Sanxin, China) of this mixture were then determined.[19] Another portion of the air-dried soil was screened using a 100-mesh sieve and then analyzed using an X-ray diffractometer (XRD; BTX-526, Olympus, Japan). Another portion (2.00 g) of air-dried soil that had been passed through a 100-mesh sieve was thoroughly mixed with 5 mL of 1.5 M hydrochloric acid. After the mixture had fully reacted, further 5 mL portions of hydrochloric acid were added until no more bubbles appeared. The sample was then centrifuged to remove the supernatant and the solid was rinsed with double-distilled (dd) water until the pH value of the rinse water was neutral. The sample was then dried at 60 °C and analyzed using an elemental analyzer (vario EL cube, Elemental, Germany) to determine the C, N, O, and S contents of the sample. The carbonate content of the soil was also determined using an acid–base titration method. The procedure involved weighing 0.1 g of soil from different groups, adding 10 mL of 0.1 mol L^{-1} HCl, shaking for 4 min, adding 2 drops of phenolphthalein reagent, and finally titrating with 0.1 mol L^{-1} NaOH solution to calculate the carbonate content.[20]

2.3 Heavy metal content of the soil and risk assessment

Portions (0.1 g) of each of the 16 air-dried soil samples were placed in polytetrafluoroethylene crucibles and digested using acid.[21,22] The metal content of the samples (lead (Pb), zinc (Zn), copper (Cu), cadmium (Cd), arsenic (As), and calcium (Ca)) was then determined by atomic absorption spectrometry (AAS; AA-
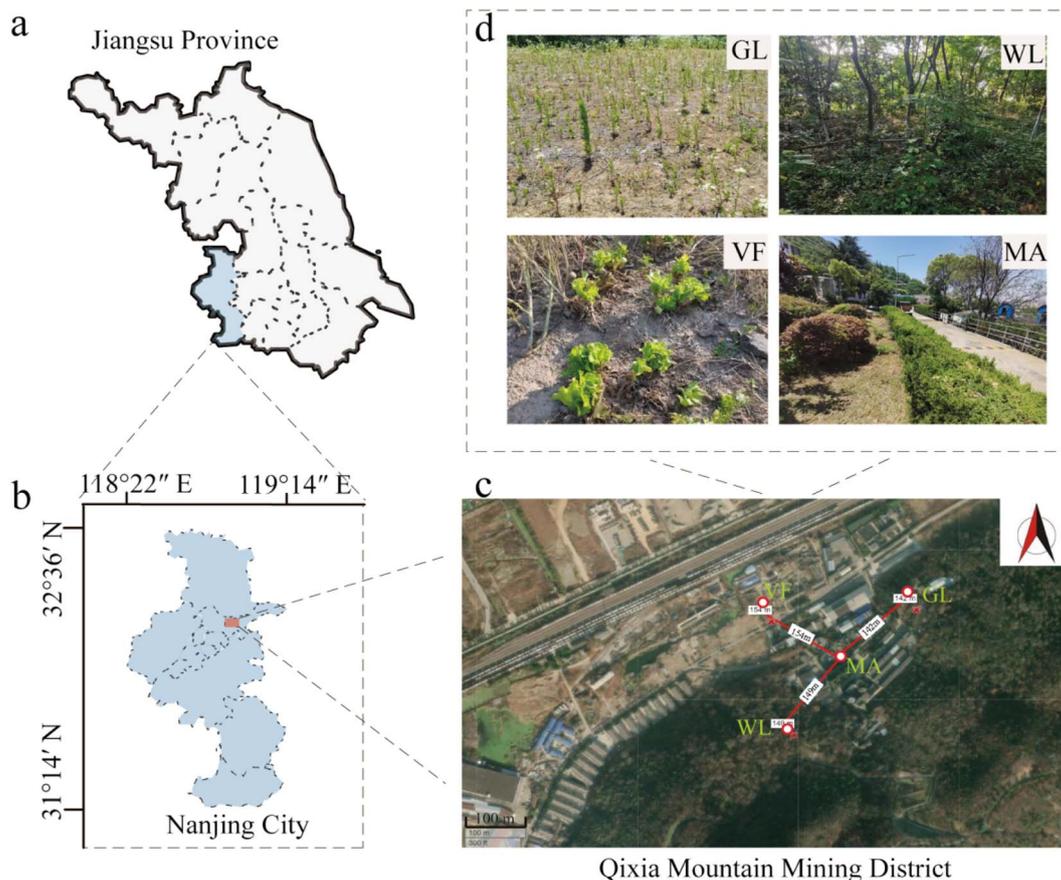
Fig. 1 Location of the sampling points selected in the Qixia Mountain lead–zinc mining area: (a) geographical location of Nanjing in Jiangsu Province. (b) Geographical location of the Qixia Mountain lead–zinc mine. (c) Distribution of the sampling points in the mining area. (d) Photographs of the vegetation covering the land in the different sampling regions.

6300C, Shimadzu, Japan). The Nemerow index is one of the most commonly used indices for assessing the risk posed to the environment by the pollution both domestically and internationally.[10] The 16 samples collected from the lead–zinc mining area in this work were therefore assessed using this index. The calculation formula of the single-factor pollution index P_i and P_N is as follows:

$$P_i = C_i/S_i$$

P_i is the pollution index of the single heavy metal element; C_i is the measured value of heavy metal content; S_i is the standard value of soil environmental quality. When the soil pH is <6.5: cadmium is less than 0.3 mg kg^{-1}, arsenic is less than 40 mg kg^{-1}, copper is less than 50 mg kg^{-1}, lead is less than 250 mg kg^{-1}, and zinc is less than 200 mg kg^{-1}; when the soil is 6.5 < pH < 7.5: cadmium is less than 0.6 mg kg^{-1}, zinc is less than 250 mg kg^{-1}, lead is less than 300 mg kg^{-1}, copper (farmland) is less than 100 mg kg^{-1} and arsenic is less than 30 mg kg^{-1}.

The calculation method of comprehensive pollution index is as follows:

$$P_N = \sqrt{\frac{\overline{P}^2 + P_{i\ max}^2}{2}}$$

P_N is the comprehensive pollution index of sampling points; P_{imax} is the maximum value of the single-factor pollution index of heavy metal pollutants at the sampling point; $P(-)$ is the average value of single-factor index. When $P_N \leq 1.0$, the soil has not been polluted, and when $P_N > 3.0$, the soil is seriously polluted.

2.4 Microbial diversity of the soil

Genomic DNA was extracted from the soil samples using DNA extraction kits (Magen, D6356-02). The extracted DNA was then diluted to 1 ng μL^{-1} with sterile water and used as a template. For bacteria, the primers used were 343F (5′-tacggraggcagcag-3′) and 798R (5′-agggtattctaatctt-3′); for fungi, ITS1F (5′-cttggtcatt-tagagaggaagtaa-3′) and ITS2 (5′-gctgcgtttcatcgatgc-3′) were used. The specific barcoding primers and a high-fidelity enzyme (TaKaRa Ex Taq, TaKaRa) were used for the PCR to ensure the efficiency and accuracy of the amplification process. The PCR products were detected using electrophoresis and purified using magnetic beads. After purification, they were used as

templates for two-round PCR amplification. The PCR products were quantified using a Qubit fluorometer after electrophoresis and purification. According to the concentration of the PCR products, the same number of samples were mixed and sequenced. According to the standard operating procedures of the Illumina NovaSeq 6000 platform (Illumina, San Diego, USA), the purified/amplified fragments were constructed into a PE2 * 250 library for sequencing (Miseq, Illumina, USA).

The microbial diversity data from the sequencing procedure were exported from the machine (in FASTQ format) for further processing. First, the Cutadapt software was used to cut off the primer sequences from the raw data sequences. Then, the DADA2 plugin was used to filter the qualified double-ended raw data from the last step according to the default parameters in the QIIME 2 (2020.11) software package. The sequences were deblurred to the same length (noise reduction) and subjected to de-chimerism and other quality control steps to obtain representative sequences and amplicon sequence variant (ASV) abundance tables. After selecting the representative sequences of each ASV using QIIME 2, all the representative sequences were compared and annotated using appropriate databases (the 16S data were aligned using the Silva 138 database, and the ITS data were aligned using the Unite database). The alignment annotations of the species were then analyzed using the q2-feature-classifier plugin (2022.11.1-2) in QIIME 2 using default parameters.

2.5 Preparation of microbial agents

Previous studies have found that *Bacillus velezensis* LB002 can induce the formation of biological vaterite with a loose and porous surface which has a good immobilization effect on heavy metals such as Pb^{2+}, Cd^{2+}, and Cu^{2+}.[23,24]

The *B. velezensis* LB002 used in this work was first activated in an LB solid medium (tryptone 1%, sodium chloride 1%, yeast powder 0.5%, agar 2%) and then inoculated into 100 mL LB liquid medium to expand the culture. A total of 18 bottles were set up and cultured at 30 °C and 180 rpm for 10 hours (at which point the optical density OD_{600} reached about 1.8). After sampling, centrifugation (5804R, Eppendorf, Germany) was performed (8000 rpm at 4 °C for 10 min). Then, bacteria in each bottle were mixed with 5 mL of a freeze-drying protective agent (a sucrose–skimmed milk powder solution consisting of 5 g sucrose, 5 g skimmed milk powder, and 100 mL of dd H_2O). They were then placed in an ultra-low-temperature refrigerator at −80 °C for 24 hours before placing in a freeze dryer (ALPHA 2-4 LD plus, Christ, Germany). At the same time, the samples of the biological source vaterite induced by *B. velezensis* LB002 were also prepared.[23]

2.6 Soil remediation experiments

2.6.1 Crop cultivation. Amaranth has a relatively short growth cycle, strong heat and drought resistance, and high nutritional value. Therefore, the crop chosen for the pot experiments in this work is amaranth. The remediation experiments were conducted using soil taken from the vegetable field (VF). The soil was naturally dried and then sieved through a 10-mesh sieve. A total of 9 groups of pots were set up (Table S1†). For each group, 6 pots were set up and the plants cultivated for 50 days. Watering was carried out regularly according to soil conditions, and no chemical or organic fertilizer was applied as the amaranth grew.

2.6.2 Plant processing. After harvesting, the amaranth plants were immediately separated into their aboveground and underground parts. First, they were rinsed with tap water, and then with distilled water 3–4 times. Filter paper was then used to absorb the surface moisture present and the lengths of the aboveground and underground parts of the amaranth measured. It was then deactivated by heating to 105 °C for 30 min, and dried to a constant weight at 65 °C. The final dry weight was recorded for each pot. The aboveground and underground parts of the dried amaranth samples were then digested, and the quantities of the heavy metals present in the different parts were determined.

2.6.3 Soil processing. Soil samples were first dried naturally to remove excess impurities, ground and passed through a 100-mesh nylon sieve. They were then mixed well, sealed in self-sealing bags, and stored. The samples were used to determine their physicochemical properties (pH, EC, carbonate content, and heavy metal content) and the crystalline forms of the minerals present. The results were then used to generate Nemerow indices for the heavy metals in the soils at the end of the pot restoration experiments.

2.7 Statistical analysis

In R version 3.5.1, we used the vegan package to analyze the alpha diversity index (Chao1, Shannon, Simpson) and β diversity, including the principal coordinate analysis (PCoA), Adonis analysis, and plot in R with the ggplot2 package. *T*-test and one-way ANOVA were performed in SPSS 20 (IBM, USA). The data are expressed as mean ± standard deviation.

3. Results

3.1 Physicochemical properties and heavy metal content of the soils

Fig. S1† shows the XRD results obtained for the soils taken from the four sampling points. The main mineral present in the GL, VF, and WL soils is quartz; the main crystalline components in the MA soil are quartz and sulfate minerals. Table 1 presents the physicochemical properties of the soil from the four different land types. As can be seen, the WL and VF soils are essentially neutral, while the GL soil is weakly alkaline and the MA soil (from around the mineral-sorting pool) is strongly acidic. The conductivity of the MA soil (3090 μs cm^{-1}) is also clearly much larger than that of the soils from the other three groups (64.5–232 μs cm^{-1}). The organic matter content of the soil (total carbon plus total nitrogen) is the largest in the WL soil and lowest in the GL soil. The highest sulfur and hydrogen contents were found in the MA soil, suggesting that the mineral-separation pool has had a direct impact on the soil in this location.

Table 1 Physicochemical properties of different soil samples (all values are expressed as mean ± SD, and the superscripts indicate results that are statistically significantly different from the others. Pollution indices (P_i) were calculated for the heavy metals in the soil samples)

Property	Sampling site			
	WL	VF	GL	MA
pH	6.87 ± 0.03^b	6.86 ± 0.08^b	7.48 ± 0.93^a	2.78 ± 0.18^c
Conductivity ($\mu s\ cm^{-1}$)	114.85 ± 23.52^b	232 ± 36.74^b	64.500 ± 12.13^b	3090 ± 287.40^a
Carbonate content (%)	0.15 ± 0.07^b	1.04 ± 0.19^a	0.91 ± 0.09^a	0^b
Total carbon (%)	3.74 ± 0.06^a	1.23 ± 0.10^b	0.31 ± 0.03^c	1.23 ± 0.09^b
Total nitrogen (%)	0.32 ± 0.014^a	0.11 ± 0^b	0.06 ± 0.01^c	0.13 ± 0.01^b
Total hydrogen (%)	0.98 ± 0.02^b	0.69 ± 0.01^c	0.718 ± 0.03^c	1.410 ± 0.07^a
Total sulfur (%)	0.08 ± 0.01^{bc}	0.11 ± 0.05^b	0.03 ± 0^c	6.54 ± 0.74^a
Calcium ($mg\ kg^{-1}$)	2010.7 ± 102.55^a	1206.7 ± 265.41^b	2086.5 ± 105.54^a	0 ± 0^c
Lead ($mg\ kg^{-1}$)	459.55 ± 47.98^b	440.38 ± 105.07^b	286.98 ± 16.08^b	1725 ± 354.76^a
Zinc ($mg\ kg^{-1}$)	1461.7 ± 162.98^a	763.32 ± 20.32^b	1433.50 ± 34.06^a	392.70 ± 59.18^c
Copper ($mg\ kg^{-1}$)	305.95 ± 16.85^a	206 ± 11.74^b	300.40 ± 0.43^a	214.42 ± 28.74^b
Cadmium ($mg\ kg^{-1}$)	1.60 ± 0.00^a	1.54 ± 0^b	1.51 ± 0^c	1.55 ± 0.01^b
Arsenic ($mg\ kg^{-1}$)	795.40 ± 74.18^b	127.83 ± 63.60^c	822.75 ± 55.16^b	1388.3 ± 408.66^a
P_i (Pb)	3.83	3.67	2.39	24.64
P_i (Zn)	5.85	3.05	5.73	1.96
P_i (Cu)	3.06	2.06	3.00	4.29
P_i (Cd)	5.34	5.14	5.01	5.15
P_i (As)	26.51	4.26	27.43	34.71
P_N	19.78	4.45	8.71	26.50

Table 1 also shows that the carbonate content of the VF and GL soils is high, while carbonate could not be detected in the MA samples. It is possible that the high levels of carbonate minerals in these soils may effectively reduce their heavy metal content. According to Tables 2 and S1,† the soils are heavily polluted with Pb, Zn, Cu, Cd, and As (with the highest pollution levels corresponding to Pb and As). The comprehensive Nemerow pollution indices for the VF and GL soils are small (Table S2†). The pollution around the mineral-flotation tank (MA) and surrounding woodland (WL) is particularly serious (Nemerow indices of 26.50 and 19.78, respectively).

3.2 Microbial diversity analysis

3.2.1 Sequencing statistics.
The sequencing experiments revealed the distributions and potential functions of the important microbial communities in the heavily polluted soils. After sequencing and performing machine quality control, the number of ASVs in the samples was distributed between 786 and 1787. ANOVA tests were then performed on the project samples to explore the statistical differences present. The number of ASVs in the samples ranged from 150 to 659 in the fungal samples. The project samples were then subjected to ANOVA testing, resulting in 337 different ASVs, 87 different genera, and 5 different gates. Table S3† shows the details of the pre-processed data obtained for the bacteria and fungi in each sample.

3.2.2 Microbial diversity results: composition and structure.
The diversity of the species present in a biological environment can be specified using alpha diversity indices. In this work, we consider four different measures of alpha diversity: the observed species (Sobs), Shannon, Simpson, and Chao1 indices, as shown in Table 2.

The alpha diversity of the bacteria at the VF and WL sites can be seen to be significantly higher than that at the GL and MA sites (according to all of the aforementioned indices). The diversity at the MA site was the lowest of all those tested, which may be related to the level of the heavy metal pollution present there. That is, it appears that the more serious the heavy metal pollution level, the lower the corresponding diversity index.

In contrast, the soil type with the highest fungal diversity is that from the WL site. The soils from the other three sites have

Table 2 Diversity (α distribution) of the bacteria and fungi in different soil samples

|	Sample	Sobs	Shannon	Simpson	Chao1
Bacteria	GL	1348.10 ± 366.83^a	8.84 ± 0.47^b	0.99 ± 0.00^b	1356.60 ± 368.08^a
	MA	1319.70 ± 367.65^a	8.40 ± 0.30^b	0.99 ± 0.00^c	1327.70 ± 372.16^a
	VF	1668.40 ± 117.73^a	9.61 ± 0.10^a	1.00 ± 0.00^a	1676.10 ± 118.85^a
	WL	1600.80 ± 97.50^a	9.42 ± 0.14^a	1.00 ± 0.00^a	1611.70 ± 97.39^a
Fungi	GL	236.2 ± 52.76^b	4.08 ± 0.90^b	0.79 ± 0.14^a	236.69 ± 53.06^b
	MA	253.32 ± 84.15^b	3.70 ± 0.48^b	0.80 ± 0.04^a	253.71 ± 84.16^b
	VF	191.38 ± 40.66^b	3.37 ± 0.45^b	0.79 ± 0.09^a	192.16 ± 40.41^b
	WL	572.45 ± 117.08^a	5.92 ± 1.43^a	0.88 ± 0.15^a	573.44 ± 116.62^a
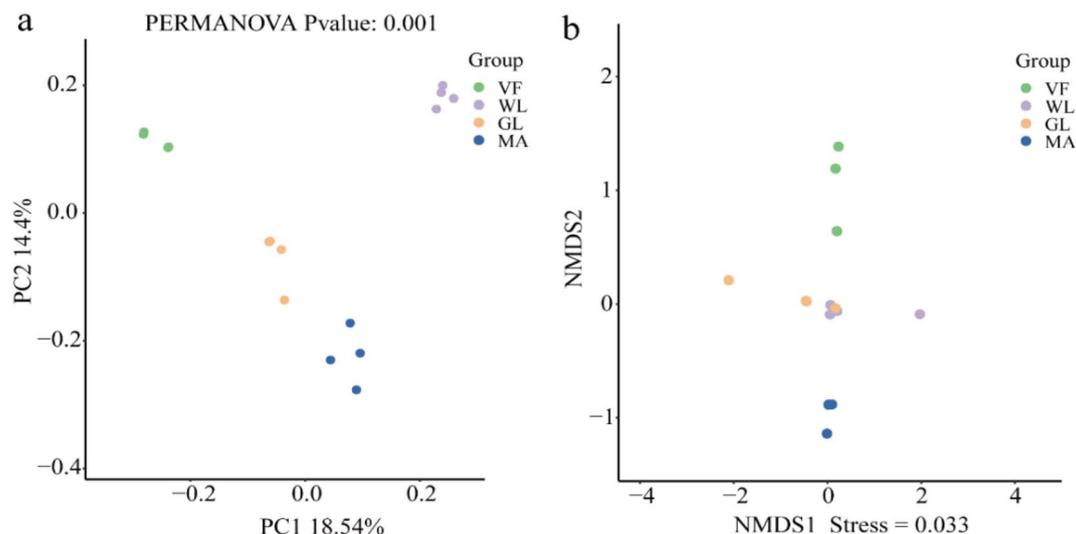
Fig. 2 Distribution of the bacterial and fungal β diversities in the samples: (a) PCoA analysis of the bacteria and (b) NMDS analysis of the fungi.

much lower fungal diversities and the differences between them are rather small.

The degree of microbial diversity between habitats is usually measured using beta diversity. In this respect, the bacteria in different groups of samples are commonly compared using principal coordinate analysis (PCoA), whereas non-metric multidimensional scaling (NMDS) analysis is commonly used for fungi. Fig. 2 shows a comparison of the beta diversities of the four groups of soil samples. As can be seen in Fig. 2a, the bacterial groups can be readily distinguished from each other using PCoA. However, the composition of the fungal colonies in the GL and WL groups are similar. The VF and MA groups were clearly affected by farming and mineral processing activity, respectively, which made them significantly different from the other groups (Fig. 2a and b).

Bacteria belonging to the phyla proteobacteria, bacteroidota, and actinobacteriota were found to be most abundant across all the samples (Fig. 3). Nitrospirota were found to be most abundant in the MA group and Firmicutes more abundant in the MA and GL groups. The fungal statistics show that ascomycota form the most widely distributed type of fungi in the four groups. Basidiomycota are also fairly abundant in the GL soil and zygomycota are most likely to be found in the MA soil.
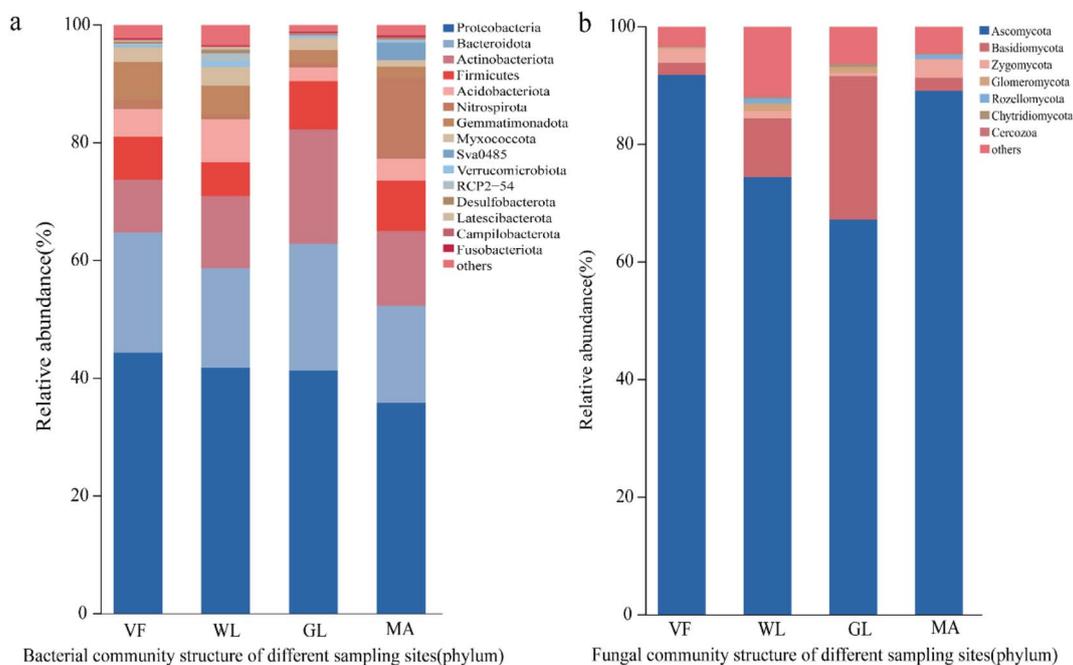

Fig. 3 Phylum level distribution of the bacteria and fungi in the microbial communities.

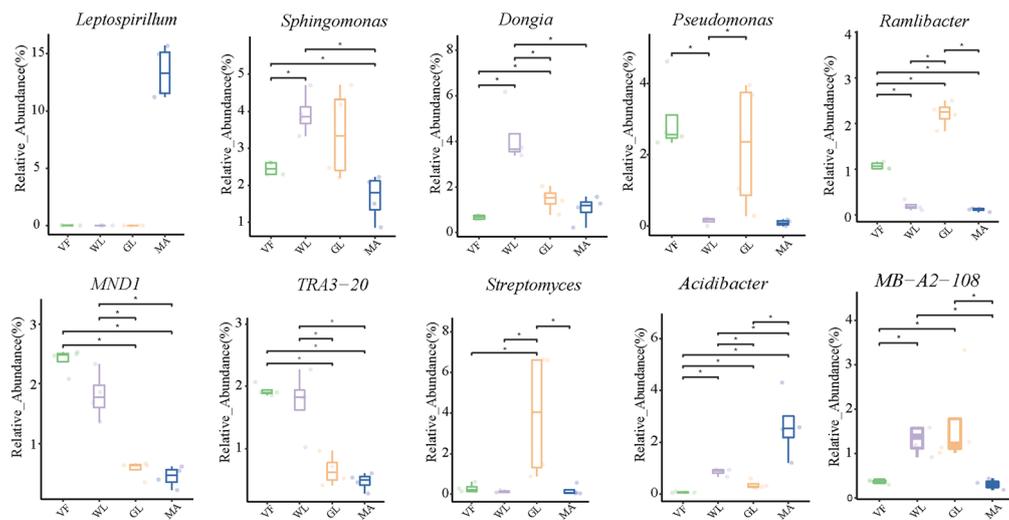© 2025 The Author(s). Published by the Royal Society of Chemistry

Fig. 4 Distribution of different bacterial flora in the soil samples.

The distribution of the dominant bacterial strains can be obtained by screening the significantly different bacterial communities in different comparative groups (Fig. 4). *Leptospirillum*, which occurs in the highest abundance in the MA group, is known to be a strain that is resistant to heavy metals. However, *Leptospirillum* is likely to have been introduced artificially for bioleaching purposes, and given that MA is located far from residential areas, its impact on human health is minimal. *Sphingomonas* is a stress-resistant strain and occurs in high abundance in all four groups. *Dongia* species have the ability to fix nitrogen and are most widely distributed in the WL soil. *Pseudomonas* is most widely distributed in the VF and GL soil. MND1 (co trophic) β-protein bacteria and TRA3-20 (belonging to Proteobacteria) have higher abundance in VF and WL. *Dongia*, *Sphingomonas*, *Pseudomonas*, MND1 (co-trophic) β-protein bacteria, and TRA3-20 possess the potential to promote plant growth and enhance soil fertility, and their ecological functions may indirectly benefit human health by maintaining soil health. *Streptomyces* is only distributed in the GL group, while acidophilic bacteria are most abundant in MA (which is related to the low pH of this soil). *Streptomyces* is a common probiotic, while acidophilic bacteria help stabilize

the acidic soil environment to some extent, reflecting the selective impact of soil acidification on microbial communities.

The distribution of the dominant fungal genera is shown in Fig. 5. The dominant genus in the WL group is *Pseudorobillarda* (*Pseudotrichomonas*). The dominant genera in the VF group are *Monographella* (*Clostridium*) and *Acremonium* (*Cladosporium*), which are common endophytic fungi in plants.[25,26] The dominant genus of fungi in the GL group is *Pyrenochaeta*, which, as an endophytic fungus in plants, has the ability to inhibit harmful fungi.[21,27,28] The four above-mentioned fungi are less abundant in MA. The presence of these plant endophytes indicates their roles in plant health and soil ecology, and their impact on human health is minimal.

The relationships between the composition of the microbial community in the different samples and different environmental factors can be investigated using redundancy analysis (RDA). The analysis performed in this work was based on a single peak model and involved 10 environmental factors. The five environmental factors that fitted the model, namely pH, Pb^{2+}, EC, total hydrogen (TH), and total sulfur (TS), were then correlated with the compositions of the bacterial communities, giving the results shown in Fig. 6. As can be seen, the
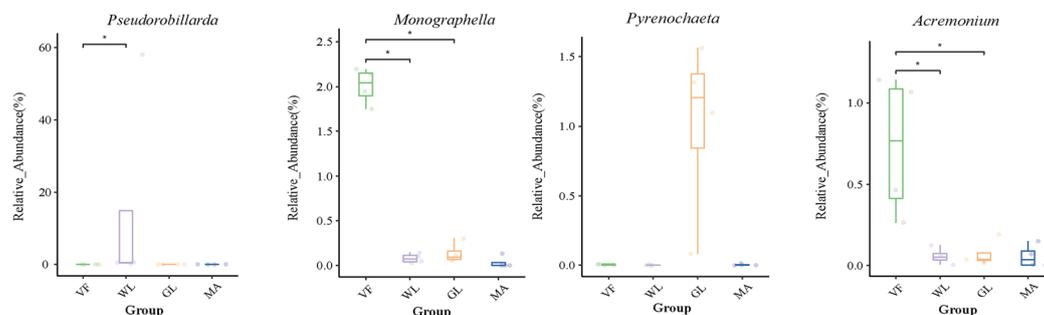

Fig. 5 Distribution of different fungal communities in the soil samples.
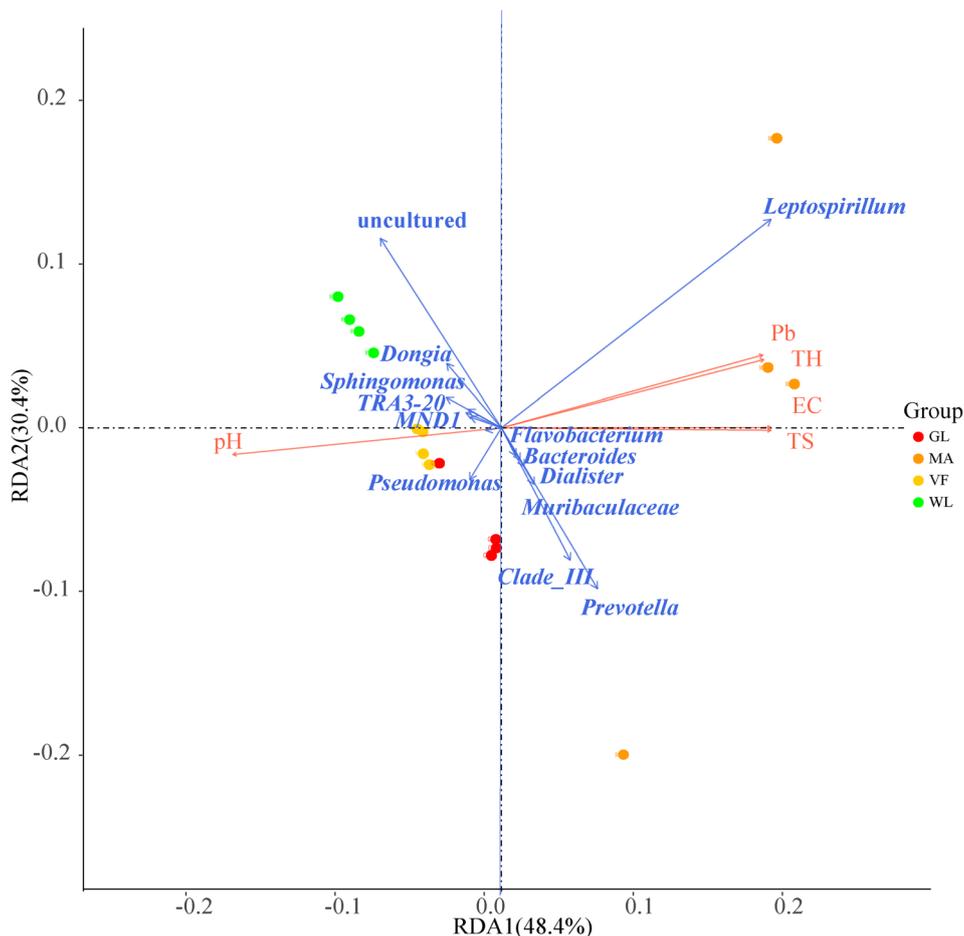
Fig. 6 Analysis of the association between environmental factors and bacterial communities.

interpretation rate of the RDA1 axis in the figure is 48.4%, and the interpretation rate of the RDA2 axis is 30.4%.

As illustrated in Fig. 6, the MA samples are distributed in the first and fourth quadrants, while the other three groups of samples are distributed in the second and third quadrants. Moreover, the MA group is positively correlated with the environmental factors Pb^{2+}, EC, TH, and TS, and negatively correlated with pH. Furthermore, the other three groups are positively correlated with pH. High concentrations of heavy metals in the soil have a significant impact on the bacterial communities in the soil. In particular, *Leptospirillum*, *Prevotella*, and Clade_III (Swedish *Campylobacter* genus) are the bacteria most correlated with the group MA. The non-pathogenic genera *Pseudomonas*, *Dongia*, and *Sphingomonas* have a greater correlation with the other three groups of samples. Due to the CCA analysis model constructed by fungi, the significance of environmental factors and microbial community distribution was not obvious, so no further analysis was performed.

3.3 Pot experiments

3.3.1 Plant growth statistics. The amaranth plants grown in the pots showed quite different rates of growth (Fig. S2†). The amaranth did not grow when 0.8% $CaCl_2$ was added to soil (Fig. 7, group D2 and S2, group D1†). The amaranth plants in the

untreated vegetable soil had the next-worst rate of growth (Fig. S2, group A1†), poorer than those grown in the soil with 0.4% $CaCl_2$ added (Fig. S2, group C1 and C2†).

The best plant growth occurred in the soil treated with bacterial agents (Fig. S2, group A2 and B2†) and biological minerals (Fig. S2, group A3†), followed by the soil treated with only 0.2% $CaCl_2$ (Fig. S2, group B1†). It can thus be seen that adding a small amount of $CaCl_2$ and bacterial agents can improve the growth of amaranth plants, while the addition of excessive amounts of $CaCl_2$ ($\geq$0.4%) may stress the amaranth and inhibit its growth.

Fig. S3† shows a more quantitative assessment of the amaranth growth observed in the A, B, and C groups of pots (aboveground and underground parts). The results show that the aboveground parts and total plant lengths of the amaranth in pots A2, A3, B1, and B2 were the longest; the plants in pots C1 and C2 were slightly shorter (Fig. S3a–c†). The aboveground and root parts of the plants in the untreated soil (A1) were the shortest.

The dry-weight results are consistent with the plant height results (Fig. S3d†). In particular, the dry weight of the plants grown in the untreated soil (A1) is significantly lower than that of the plants in the other groups. In addition, the dry weight of the plants grown in the soil treated with 0.4% $CaCl_2$ is lower
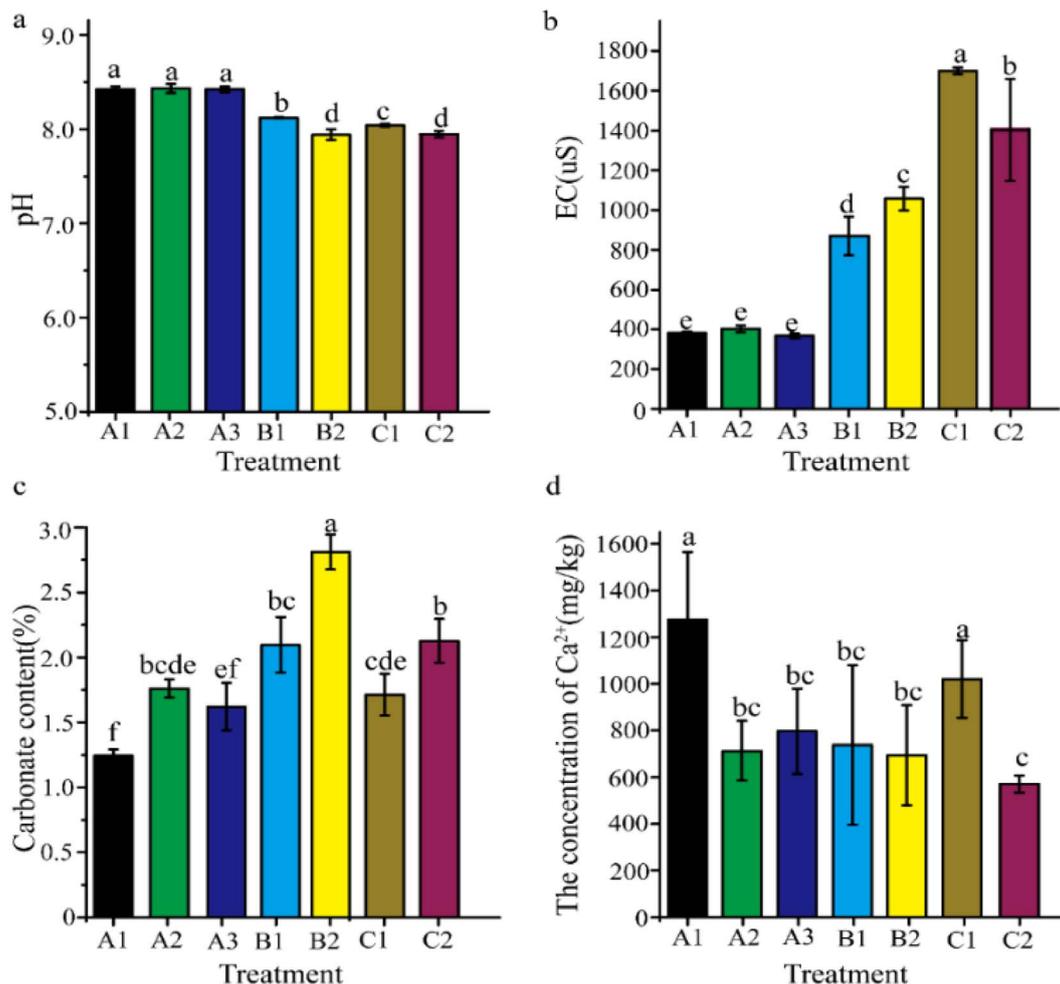
Fig. 7 Physical and chemical properties of the soils after the completion of pot experiments: (a) pH, (b) EC, (c) carbonate content, and (d) Ca^{2+} content.

than that found for other plants grown in soil treated with smaller amounts of $CaCl_2$ or even none at all.

The edible (aboveground) parts of the amaranth plants were found to contain no Pb, Cd, or As, but Zn, Cu, and Ca were present in the quantities shown in Table S3.† Of these, the Cu contents of the different plants are all less than the safe value limit (10 mg kg^{-1}). The amounts of Zn^{2+} and Ca^{2+} present are higher, but there are no relevant standards associated with these elements (Zn and Ca are essential metal elements for the human body). In the groups A1–A3 (soil not receiving $CaCl_2$), the high Zn^{2+} content may pose some risk. However, there is a positive correlation between the Zn^{2+} and Ca^{2+} contents and there is no risk associated with adding Ca^{2+}.

The variation of the Zn^{2+} content in the roots of the amaranth (Table S5†) is opposite to that in the edible parts, indicating that the Zn^{2+} ions are more readily transported upwards in the plant (Table S5†). The Cu^{2+} content of the root parts is low but the Ca^{2+} content is high, indicating that the roots become enriched in calcium much more readily.

3.3.2 Analysis of the soil samples. Fig. 7 shows the properties of the soils in the pots at the end of the soil remediation experiments. As can be seen, the pH of the soil changed from neutral to alkaline (Fig. 7a), the soil conductivity (EC) gradually increased with the addition of Ca^{2+} (Fig. 7b), and the soil carbonate content also increased (Fig. 7c). Among the latter, the increase in group B2 was the most significant (from 1.04% to 2.66%) and the carbonate in the group A1 increased by at least 1.24%. The addition of the bacterial agent significantly increased the carbonate content of the soil (Fig. 7c).

The Ca^{2+} content of the soil was found to be highest in the groups A1 and C1 and much lower in the other groups (Fig. 7d). This may be related to the reasonable growth of the plants in these pots and the amount of Ca^{2+} absorbed by the plants.

After remediation, the heavy metal pollution indices of the soils decreased significantly (Table 3). Based on the evaluation criteria, that is pH > 7.5, the comprehensive pollution indices calculated for the heavy metals in each group are deemed to correspond to warning values. The highest single-factor pollution index was found for Pb. The single-factor pollution index for Zn was slightly lower (except for group A3 which is 1.34), and the Cu index corresponds to soil that is no longer polluted. The P_N indices obtained for the groups A2, B2, and C2 (i.e. with biological agents added) were the smallest calculated.

Table 3 Heavy metal contents in soil samples at the end of the remediation experiments and the corresponding P_N values

Group	Heavy metal content (mg kg^{-1})			Pollution indices P_N			
	Pb^{2+}	Zn^{2+}	Cu^{2+}	Pb	Zn	Cu	P_N
A1	201.68 ± 87.87[ab]	348.48 ± 56.34[b]	48.76 ± 20.06[a]	1.19	1.16	0.49	1.07
A2	153.14 ± 16.88[b]	140.00 ± 54.29[e]	0[c]	0.90	0.46	0	0.70
A3	199.85 ± 58.92[ab]	402.33 ± 2.71[ab]	3.58 ± 2.78[c]	1.18	1.34	0.04	1.12
B1	194.81 ± 38.48[ab]	282.88 ± 42.41[c]	40.35 ± 26.88[ab]	1.15	0.94	0.40	1.00
B2	186.57 ± 28.20[ab]	227.23 ± 11.77[cd]	40.66 ± 9.14[ab]	1.10	0.76	0.41	0.94
C1	173.29 ± 0.80[b]	169.01 ± 71.26[de]	63.79 ± 23.16[a]	1.10	0.56	0.64	0.94
C2	171.45 ± 5.55[b]	150.75 ± 6.84[e]	23.50 ± 6.65[bc]	1.01	0.50	0.24	0.82

The crystal forms of the minerals in the soil did not change much as a result of the remediation experiments, the important component remaining quartz (Fig. S4†).

4. Discussion

4.1 Heavy metal pollution and microbial ecological distribution characteristics

The soil around the Qixia Mountain lead–zinc mine contains different concentrations of heavy metals due to the mining carried out at the mine and subsequent transportation of metal minerals. All of the soils tested were found to be seriously polluted (Table S2†).

The land used to grow vegetables (VF) has clearly been affected by the farming activities carried out at such sites. As a result, it produced the lowest heavy metal pollution index in our tests (Table S2†). The WL site has, over the years, hosted various forms of vegetation, creating a rich biodiversity and resulting in the highest total carbon and nitrogen content measured in our experiments (Table 1). As the WL site is located in the scenic Qixia Mountain area, there is no need to reclaim this land to plant other crops. It therefore poses little risk to the residents in the area.

The GL site is subject to soil compaction, resulting in low organic carbon and nitrogen content. Its heavy metal pollution index is also high. The wild grass growing in the GL site is mainly *Conyza canadensis*, which does not have beneficial effects on the soil conditions that may help cultivate other crops (Fig. 1d). Although the content of the organic matter in the VF site around the lead–zinc mine is high, the excessive amounts of heavy metals present will make it more difficult to grow crops. Considering the results of the pot experiments (Table S5†), it can be expected that plants grown in the VF soil will become enriched in high quantities of Zn^{2+}. Therefore, the VF soil near the mine needs to be improved. The microbial communities that occur in nature generally contain a wide distribution of dominant species and a few rarer species that can adapt to the specific environment encountered.[29,30] The microbial diversity in the different types of soil in the Qixia Mountain lead–zinc mine area has clearly been affected by heavy metal pollution.

The abundance of bacterial communities was higher in the WL and VF soils (Table S3†). Plants grown in the WL soil grew vigorously and the VF soil was the least polluted in this work (yielding the smallest heavy metal pollution index value). Therefore, the Shannon and Simpson bacterial diversity indices for these soils are significantly higher than those of the other two groups. The differences between the Chao1 indices of the four groups are slightly smaller because this index is more sensitive to rare species (so the difference in the richness of the bacterial species in the four groups is small). Heavy-metal stress can increase the number of endemic or uncertain species in a soil's microbial community. For example, Rastogi *et al.* found that the number of unknown sequences of 16S rRNA amplicons in the bacterial community present in sediment from the Coeur d'Alene River (in Idaho, USA) increased due to the effect of heavy-metal-induced stress.[31]

Bacteria belonging to the *Proteobacteria*, *Bacteroidota*, and *Actinobacteriota* phyla were found to be most abundant in each plot. These phyla have also been reported to be dominant in other different types of soil.[32] The resistance of microbes to heavy metal pollution and their ability to function are affected by many factors. These include how easy it is for heavy metal-resistant strains to replace more sensitive strains, how readily genes can be transferred to maintain their resistance to heavy metals, and how long the heavy metals continue to be available for.[33] Proteobacteria belonging to the genus *Sphingomonas* have been found to be resistant to heavy metals and were found in the WL, GL, and VF soils in this work. They can therefore be applied to the remediation of soil contaminated with heavy metal pollution.

Unlike bacteria, fungi play an indispensable role in decomposing the insoluble organic matter in soil and thus promoting element cycling. In the case of heavy metals, the fungal communities in different soil samples were found to be significantly different. The forest ecosystem (WL soil) appeared to contain the most complex system in our work. Its dominant genus *Pseudorobillarda* can produce a variety of secondary metabolites with metabolic activity. It thus has antibacterial activity and is conducive to maintaining and promoting plant growth. Similarly, *Mortierella*, the dominant genus in the VF soil, has also been shown to promote plant growth. The distribution of *Biscogniauxia* and *Acidomyces* (the dominant fungi in the MA soil near the mineral-sorting pool) is strongly influenced by the acidic nature of the soil. *Biscogniauxia* plays an important role in the degradation of lignocellulose, nutrient cycling, and secondary-metabolite production. *Acidomyces* is a strain

commonly used to treat acidic wastewater (with a pH of ~2). As the heavy metal resistance of fungi is stronger than that of bacteria, fungal community distributions are not just affected by heavy metal pollution levels, but also by the pH of the soil and varieties of plants present.

The mineral mining and separation processes directly affect the pH, heavy metal content, and microbial composition of the surrounding soil. Our correlation analysis of the various environmental factors shows that the low pH and high electrical conductivity of the soil around the mineral separation tank (Table 1) cause a large change in the bacterial distribution in the MA soil compared to the other three groups of soil. As the soil is highly acidic and heavily contaminated with Pb^{2+}, the dominant bacteria in the MA soil samples were *Leptospirillum* and *Prevotella*. *Leptospirillum* is eosinophilic and grows optimally when the pH is in the range of 1.5–1.8. *Prevotella*, which can ferment sugar to produce acetic and succinic acids,[34] can survive in environments with pH values of 4.5. The other genera were significantly less common in the MA soil group. Apart from its high heavy metal content, it is the acidity of the environment (low pH) that is responsible for this.[35] For example, heavy-metal-resistant strains of *Sphingomonas* are not prominent in the MA group (but they are found in the other three groups which have lower pollution indices) because the *Sphingomonas* species cannot thrive in this highly acidic soil. *Pseudomonas* and *Dongia* contain genes that allow them to resist the presence of heavy metals.[36,37] As a result, they have been preliminarily applied in the remediation of soil contaminated with heavy metals. These two genera will therefore have an obvious advantage over other species in the VF, GL, and WL soils (which have slightly lower heavy metal pollution levels).

In summary, we believe that heavy metal pollution will cause great changes in the microbial flora present in contaminated soil. More specifically, strains that are resistant to heavy metal pollution will increase in abundance significantly. Soil that is strongly acidic as well as polluted with heavy metals will experience a decrease in the abundance of resistant strains. Clearly, this is not conducive to the remediation of soil heavily contaminated with heavy metals.

4.2 Remediation of contaminated soil using plant–microorganism synergy

The use of microbe-induced mineralization to remediate soil polluted with heavy metals has been the fastest-growing method of bioremediation in recent years.[38–40] Due to the high levels of heavy metals present in the vegetable field (VF) in the mining area, a large number of crop plants were found to be short, clearly finding it difficult to grow (Fig. 1d and 7, group A1). However, in our remediation experiments, the addition of freeze-dried *B. velezensis* had an obvious growth-promoting effect on the amaranth plants. The addition of a small amount of $CaCl_2$ (~0.2%) also promoted plant growth (Fig. 7, group B2 and S2B1†). However, the addition of a larger amount of $CaCl_2$ (>0.4%) inhibited the growth of the amaranth plants (Fig. S2†). This would not only be a waste of resources but may also cause soil compaction. Therefore, in the mining area, the

application of freeze-dried *B. velezensis* may well be able to promote crop growth.

In addition to favorable growth rates, the uptake of heavy metals by the crops is another important issue. In our experiments, the amaranth plants did not assimilate Cd, Pb, As, and other heavy metal ions from the soil. The uptake of Cu^{2+} is not very significant (and therefore not a health risk) and the amount of Ca^{2+} in the plants is not too high and is harmless to the human body anyway. However, their Zn^{2+} content is high and needs to be addressed (Table S4†). By adding a small amount of $CaCl_2$, the absorption of Zn^{2+} by the plants could be reduced, especially in the edible parts aboveground. *B. velezensis* has been shown to improve the soil environment and promote plant growth.[41] In this work, the *B. velezensis* microbial agent was able to improve the amaranth crop produced, so that it met the standards required for it to be deemed edible. Therefore, *B. velezensis* is clearly a promising candidate for application in controlling heavy metal pollution in soils.

4.3 Pollution state near the lead–zinc mine and control measures

The heavy metal pollution indices calculated for the different types of soil in the Qixia Mountain lead–zinc mining area suggest that the most serious pollution is, not surprisingly, in the soil near the mineral-sorting pool (MA). If this soil is taken to be at the epicenter of our study area, then the other sampling sites (WL, VF, and GL) are almost equidistantly distributed around this epicenter (Fig. 1c). These three plots are also polluted to varying degrees (Fig. 8).

The heavy metal pollution has caused the dominant microbial strains in the four types of soil to be very similar (Fig. 8). The soil used to grow vegetables in this study was collected from a vegetable field adjacent to the mineral-separation pool. As the farm is located in an area known to contain lead and zinc ores, the soil itself may naturally contain high levels of heavy metal ions. Of course, it would have also been affected by its long-term exposure to the mineral processing and transportation activity that took place nearby. This might well have aggravated its heavy metal pollution status.

After remediating the vegetable field using a combined plant–microorganism treatment regime, its heavy metal content was greatly reduced. The biological agent improved the soil's pollution state by inducing carbonate mineralization (Fig. 8). By greatly improving the carbonate content of the soil, the heavy metal content absorbed by plants was reduced, thus promoting the plant growth. However, attention must be paid to the amount of Ca^{2+} added in the remediation process as adding too much can change the structure of the soil and reduce the subsequent crop yield.

In summary, this paper revealed the effect of long-term mining activity on the pollution state of the soil surrounding the mining site and also the corresponding distribution of microorganisms in the soil. We proposed a specific scheme for treating heavily polluted soil using plants and microorganisms to induce mineralization.
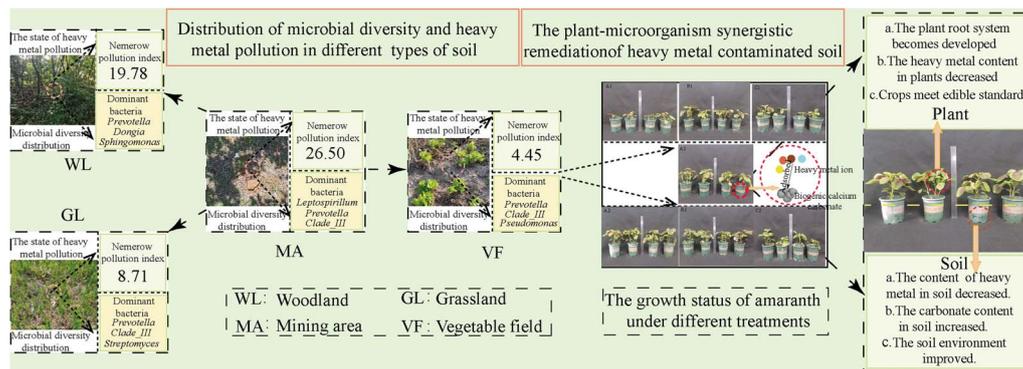
Fig. 8 Present state of the heavy metal pollution near the Qixia Mountain lead–zinc mine, and the proposed method that could be used to remediate the soil.

5. Conclusions

Long-term mining has led to a serious pollution issue in the soil around the Qixia Mountain lead–zinc mine. The WL, GL, and VF soils taken from around the mining area are still seriously polluted by heavy metals, even after more than a decade of strict control. Severe heavy metal pollution can cause significant changes in soil-microbial communities, with a significant increase in the abundance of heavy metal-resistant strains. Under heavy metal pollution, the strong acidity of the soil can lead to a decrease in resistant strains, which is not conducive to the improvement of soil heavy metal pollution. Adding *B. velezensis* and biogenic vaterite can reduce the heavy metal content of the soil, which improves the growth performance of plants growing in the agricultural soil and reduces the plants' uptake of heavy metals by the plants, rendering them pollution-free (or reducing their heavy metal content close to critical levels). This study reveals the adverse effects of long-term mining on the soil environment around the mining area. It also shows that the mineralization induced by plant–microorganism interaction can be used to remediate the damage caused by the heavy metal pollution. This study not only reveals the adverse effects of long-term mining on the surrounding soil environment, but also provides a theoretical basis for the remediation of heavy metal-contaminated soils, holding significant importance for the protection of soil ecological functions and human health.

Data availability

Data will be made available upon request.

Author contributions

Xiaofang Li: conceptualization, investigation, methodology, writing original draft. Xiaochi An: investigation, methodology. Kairui Jiao: investigation, methodology. Haoqin Pan: investigation, methodology, writing original draft. Bin Lian: conceptualization, formal analysis, data curation, writing–review & editing, supervision.

Conflicts of interest

The authors declare that they have no known competing financial interests or personal relationships that could have appeared to influence the work reported in this paper.

Acknowledgements

References

1 M. Jarolimova, D. Cechova, P. Sachova, M. Komarek, M. Prochazka and SGEM, The effect of coal mining on the environment of the town of Bilina and its Surroundings, *Proceedings of the 15th International Multidisciplinary Scientific Geoconference (SGEM), Albena, Bulgaria, Jun 18–24*, Albena, Bulgaria, 2015.

2 Y. Liu, M. Xie, J. Liu, H. Wang and B. Chen, Vegetation disturbance and recovery dynamics of different surface mining sites via the land trendr algorithm: Case study in Inner Mongolia, China, *Land*, 2022, **11**, 856.

3 M. K. Ghose and S. R. Majee, Assessment of dust generation due to opencast coal mining - An Indian case study, *Environ. Monit. Assess.*, 2000, **61**, 255–263.

4 A. Zdravkovic, V. Cvetkovic, K. Saric, A. Pacevski, A. Rosic and S. Eric, Waste rocks and medieval slag as sources of environmental pollution in the area of the Pb-Zn Mine Rudnik (Serbia), *J. Geochem. Explor.*, 2020, **218**, 106629.

5 U. Aleksander-Kwaterczak and E. Helios-Rybicka, Contaminated sediments as a potential source of Zn, Pb, and Cd for a river system in the historical metalliferous ore

mining and smelting industry area of South Poland, *J. Soils Sediments*, 2009, **9**, 13–22.

6 A. Lachhab, E. M. Benyassine, M. Rouai, A. Dekayir, J. C. Parisot and M. Boujamaoui, Integration of multi-geophysical approaches to identify potential pathways of heavy metals contamination - A case study in Zeida, Morocco, *J. Environ. Eng. Geophys.*, 2020, **25**, 415–423.

7 A. R. Vidal Jeronimo do Nascimento, G. K. Gabriel Cunha, C. W. Araujo do Nascimento and K. P. Vieira da Cunha, Assessing soil quality and heavy metal contamination on scheelite mining sites in a tropical semi-arid setting, *Water, Air, Soil Pollut.*, 2021, **232**, 375.

8 Z. Sun, X. Xie, P. Wang, Y. Hu and H. Cheng, Heavy metal pollution caused by small-scale metal ore mining activities: A case study from a polymetallic mine in South China, *Sci. Total Environ.*, 2018, **639**, 217–227.

9 W.-S. Liu, M.-N. Guo, C. Liu, M. Yuan, X.-T. Chen, H. Huot, C.-M. Zhao, Y.-T. Tang, J. L. Morel and R.-L. Qiu, Water, sediment and agricultural soil contamination from an ion-adsorption rare earth mining area, *Chemosphere*, 2019, **216**, 75–83.

10 M. Wang, L. Yang, J. Li and Q. Liang, The evaluation and sources of heavy metal anomalies in the surface soil of eastern Tibet, *Minerals*, 2023, **13**, 86.

11 E. Xiao, Z. Ning, T. Xiao, W. Sun and S. Jiang, Soil bacterial community functions and distribution after mining disturbance, *Soil Biol. Biochem.*, 2021, **157**, 108232.

12 T. Gao, X. Wang, Y. Liu, H. Wang, M. Zuo, Y. He, H. Li, G. Li, C. Li, X. Lis, X. Li and Y. Yang, Characteristics and diversity of microbial communities in lead–zinc tailings under heavy metal stress in north-west China, *Lett. Appl. Microbiol.*, 2022, **74**, 277–287.

13 X. Zhao, J. Huang, J. Lu and Y. Sun, Study on the influence of soil microbial community on the long-term heavy metal pollution of different land use types and depth layers in mine, *Ecotoxicol. Environ. Saf.*, 2019, **170**, 218–226.

14 I. Sanchez-Castro, P. Martinez-Rodriguez, M. M. Abad, M. Descostes and M. L. Merroun, Uranium removal from complex mining waters by alginate beads doped with cells of Stenotrophomonas sp. Br8: Novel perspectives for metal bioremediation, *J. Environ. Manage.*, 2021, **296**, 113411.

15 J. Guzman-Moreno, L. Fernando Garcia-Ortega, L. Torres-Saucedo, P. Rivas-Noriega, R. Maria Ramirez-Santoyo, L. Sanchez-Calderon, I. Noemi Quiroz-Serrano and L. Elena Vidales-Rodriguez, *Bacillus megaterium* HgT21: a promising metal multiresistant plant growth-promoting bacteria for soil biorestoration, *Microbiol. Spectrum*, 2022, **10**, 5, DOI: **10.1128/spectrum.00656-22**.

16 Y. Xie, H. Bu, Q. Feng, M. Wassie, M. Amee, Y. Jiang, Y. Bi, L. Hu and L. Chen, Identification of Cd-resistant microorganisms from heavy metal-contaminated soil and its potential in promoting the growth and Cd accumulation of bermudagrass, *Environ. Res.*, 2021, **200**, 111730.

17 H. Gong, Y. Qi, J. Gao, C. Lv, K. Min and T. Lan, The origin and ore-forming processes of the Qixiashan Pb-Zn-Ag deposit, South China: Constraints from LA-ICP-MS analysis

18 B.-b. Chu and L.-q. Luo, EDXRF analysis of soil heavy metals on Lead-Zinc Orefield, *Spectrosc. Spectral Anal.*, 2010, **30**, 825–828.

19 X. An, Z. Wang, X. Teng, R. Zhou, X. Wang, M. Xu and B. Lian, Rhizosphere bacterial diversity and environmental function prediction of wild salt-tolerant plants in coastal silt soil, *Ecol. Indic.*, 2022, **134**, 108536.

20 H. Fu, X. Jian, W. Zhang and F. Shang, A comparative study of methods for determining carbonate content in marine and terrestrial sediments, *Mar. Pet. Geol.*, 2020, **116**, 104337.

21 F. Zhu, X. Hu, Z. Guo and F. Mei, Determination of heavy metals in soil by rapid digestion, *Chin. J. Anal. Lab.*, 2019, **38**, 906–911.

22 S. Uchida, K. Tagami and K. Tabei, Comparison of alkaline fusion and acid digestion methods for the determination of rhenium in rock and soil samples by ICP-MS, *Anal. Chim. Acta*, 2005, **535**, 317–323.

23 R. Liu, Y. Yu, X. Liu, Y. Guan, L. Chen and B. Lian, Adsorption of Ni^{2+} and Cu^{2+} using bio-mineral: adsorption isotherms and mechanisms, *Geomicrobiol. J.*, 2018, **35**, 742–748.

24 R. Liu and B. Lian, Immobilisation of Cd(II) on biogenic and abiotic calcium carbonate, *J. Hazard. Mater.*, 2019, **378**, 120707.

25 Q. Zhao, Y. Yu and Z. Bei, Isolation and identification of fungal endophytes from Swainsona salsula grown in Ningxia, *Pratac. Sci.*, 2012, **29**, 1821–1826.

26 Y. Zheng, H. Fan, W. Chen, J. Wu, Y. Huang, Q. Zeng and Y. Huang, Isolation and identification of endophytic fungi in *Stemona tuberosa*, *Lishizhen Med. Mater. Med. Res.*, 2022, **33**, 2271–2273.

27 X. Geng, J. Shu, H. Peng and W. Zhang, Fungal communities in twigs of three bamboo species based on high-throughput sequencing technology, *Chin. J. Ecol.*, 2018, **37**, 3493–3498.

28 F. Yang, C. Liu, L. Liu, S. Wang, X. Jiang, M. Li, D. Cao and X. Li, Isolation of endophytic fungi from medicinal plants and screening for antagonistic strains, *Plant Prot.*, 2021, **47**, 78–85.

29 R. L. Bier, E. S. Bernhardt, C. M. Boot, E. B. Graham, E. K. Hall, J. T. Lennon, D. R. Nemergut, B. B. Osborne, C. Ruiz-Gonzalez, J. P. Schimel, M. P. Waldrop and M. D. Wallenstein, Linking microbial community structure and microbial processes: an empirical and conceptual overview, *FEMS Microbiol. Ecol.*, 2015, **91**, fiv113.

30 Z.-S. Hua, Y.-J. Han, L.-X. Chen, J. Liu, M. Hu, S.-J. Li, J.-L. Kuang, P. S. G. Chain, L.-N. Huang and W.-S. Shu, Ecological roles of dominant and rare prokaryotes in acid mine drainage revealed by metagenomics and metatranscriptomics, *ISME J.*, 2015, **9**, 1280–1294.

31 G. Rastogi, S. Barua, R. K. Sani and B. M. Peyton, Investigation of microbial populations in the extremely metal-contaminated coeur d'Alene sediments, *Microb. Ecol.*, 2011, **62**, 1–13.

32 M. Chodak, M. Golebiewski, J. Morawska-Ploskonka, K. Kuduk and M. Niklinska, Diversity of microorganisms

from forest soils differently polluted with heavy metals, *Appl. Soil Ecol.*, 2013, **64**, 7–14.

33 B. S. Griffiths and L. Philippot, Insights into the resistance and resilience of the soil microbial community, *FEMS Microbiol. Rev.*, 2013, **37**, 112–129.

34 M. Yanagisawa, T. Kuriyama, D. W. Williams, K. Nakagawa and T. Karasawa, Proteinase activity of Prevotella species associated with oral purulent infection, *Curr. Microbiol.*, 2006, **52**, 375–378.

35 E. Xiao, Y. Wang, T. Xiao, W. Sun, J. Deng, S. Jiang, W. Fan, J. Tang and Z. Ning, Microbial community responses to land-use types and its ecological roles in mining area, *Sci. Total Environ.*, 2021, **775**, 145753.

36 S. K. Kim, C. G. Lee and H. S. Yun, *Dongia* soli sp nov., isolated from soil from Dokdo, Korea, *Antonie van Leeuwenhoek J.*, 2016, **109**, 1397–1402.

37 C.-Y. Lu, L. Dong, D. Wang, S. Li, B.-Z. Fang, M.-X. Han, F. Liu, H.-C. Jiang, I. Ahmed and W.-J. Li, Isolated from the Gurbantunggut Desert Soil, *Curr. Microbiol.*, 2022, **79**, 342.

38 A. Bhattacharya, S. N. Naik and S. K. Khare, Harnessing the bio-mineralization ability of urease producing *Serratia marcescens* and *Enterobacter cloacae* EMB19 for remediation of heavy metal cadmium (II), *J. Environ. Manage.*, 2018, **215**, 143–152.

39 C.-H. Kang and J.-S. So, Heavy metal and antibiotic resistance of ureolytic bacteria and their immobilization of heavy metals, *Ecol. Eng.*, 2016, **97**, 304–312.

40 J. Cheng, Z. Sun, Y. Yu, X. Li and T. Li, Effects of modified carbon black nanoparticles on plant-microbe remediation of petroleum and heavy metal co-contaminated soils, *Int. J. Phytorem.*, 2019, **21**, 634–642.

41 A. Afzal, S. Bahader, T. Ul Hassan, I. Naz and A. Z. Din, Rock phosphate solubilization by plant growth-promoting *Bacillus velezensis* and its impact on wheat growth and yield, *Geomicrobiol. J.*, 2023, **40**, 131–142.